

Unveiling the Tapestry: the Interplay of Generalization and Forgetting in Continual Learning

Zenglin Shi*, Jie Jing*, Ying Sun, Joo Hwee Lim, Mengmi Zhang†

*Equal contribution †Corresponding author

Abstract—In AI, generalization refers to a model’s ability to perform well on out-of-distribution data related to the given task, beyond the data it was trained on. For an AI agent to excel, it must also possess the continual learning capability, whereby an agent incrementally learns to perform a sequence of tasks without forgetting the previously acquired knowledge to solve the old tasks. Intuitively, generalization within a task allows the model to learn underlying features that can readily be applied to novel tasks, facilitating quicker learning and enhanced performance in subsequent tasks within a continual learning framework. Conversely, continual learning methods often include mechanisms to mitigate catastrophic forgetting, ensuring that knowledge from earlier tasks is retained. This preservation of knowledge over tasks plays a role in enhancing generalization for the ongoing task at hand. Despite the intuitive appeal of the interplay of both abilities, existing literature on continual learning and generalization has proceeded separately. In the preliminary effort to promote studies that bridge both fields, we first present empirical evidence showing that each of these fields has a mutually positive effect on the other. Next, building upon this finding, we introduce a simple and effective technique known as Shape-Texture Consistency Regularization (STCR), which caters to continual learning. STCR learns both shape and texture representations for each task, consequently enhancing generalization and thereby mitigating forgetting. Remarkably, extensive experiments validate that our STCR, can be seamlessly integrated with existing continual learning methods, where its performance surpasses these continual learning methods in isolation or when combined with established generalization techniques by a large margin. Our data and source code will be made publicly available upon publication.

Index Terms—Continual learning, Generalization, Robustness, Shape-texture bias

I. INTRODUCTION

ARTIFICIAL intelligent agents must possess the capability not only to learn and recognize out-of-distribution data related to a given task but also to excel at continual learning, acquiring knowledge over a sequence of tasks without forgetting information from earlier tasks. Both these capabilities are crucial for the deployment of AI in dynamically changing and complex environments. Consider an autonomous vehicle journeying from California to Boston in the US, where it encounters varying weather conditions, transitioning from sunny

to snowy. Additionally, the vehicle may come across novel objects along the route, requiring continuous learning to detect these new objects without forgetting the previously learned ones. While both generalization and continual learning are essential for an AI agent, these two areas have largely been studied in isolation within existing literature.

In Artificial Intelligence (AI), generalization refers to a challenging setting where a model has to perform well on out-of-distribution data related to the given task beyond the data it was trained on. Existing solutions for out-of-domain generalization often rely on increasing data diversity. This includes data augmentation techniques like MixUp [1], AugMix [2], shape and texture representation learning [3], and adversarial training [4].

Concurrently, in the continual learning setting, agents are tasked with incrementally learning a sequence of tasks without experiencing catastrophic forgetting of the in-distribution data of earlier tasks. This challenge of catastrophic forgetting has led to the development of regularization-based approaches *e.g.*, [5]–[12]. These methods aim to preserve essential parameters for old tasks through knowledge distillation or heuristics. Replay-based approaches, *e.g.*, [9], [10], [13]–[16], involve storing or synthesizing exemplars from old tasks to train alongside new ones. More recently, architecture expansion methods, *e.g.*, [17], have emerged, altering the model structure or tuning the learnable prompts to accommodate new tasks.

In our initial efforts to explore the interplay between generalization and forgetting within continual learning, we conduct a comprehensive study. This involves the direct integration of existing generalization methods with continual learning baselines, followed by an evaluation of these integrated models. We assess their performance in terms of forgetting about earlier tasks and handling out-of-distribution data from all the tasks trained so far (**Fig. 1**). Remarkably, empirical evidence from our study indicates a mutually beneficial relationship between generalization and continual learning capabilities. Specifically, continual learning methods exhibiting reduced forgetting showcase enhanced generalization for all the previous tasks and the current task. Conversely, a superior generalization method contributes to a reduction in forgetting when it comes to earlier tasks. These findings underscore the intricate and reciprocal relationship between the two fundamental capabilities in AI.

Building upon this finding, we further enhance the existing generalization and continual learning baselines by introducing a simple yet effective Shape Texture Consistency Regularization method, dubbed STCR. In every current task, STCR distills

ZS is with Agency for Science, Technology and Research (A*STAR), Institute for Infocomm Research (I2R), Singapore

JJ is with Nanyang Technological University (NTU), A*STAR I2R, A*STAR Center for Frontier AI Research (CFAR), and Sichuan University.

YS and JL are with A*STAR I2R and CFAR.

MZ is with NTU, A*STAR I2R and CFAR

Address correspondence to mengmi.zhang@ntu.edu.sg

Manuscript received mm-dd-yyyy; revised mm-dd-yyyy.

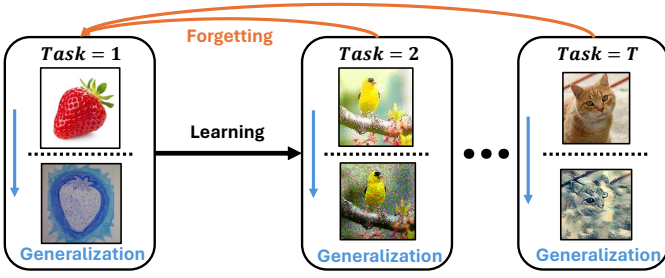


Fig. 1: **Illustration of the interplay between out-of-distribution generalization and continual learning.**

Over successive tasks, the model incrementally learns to recognize new object classes (black arrows), such as strawberries in Task 1 followed by birds in Task 2, and so on. During this continual learning process, the model exhibits a progressive loss of previously acquired knowledge known as catastrophic forgetting (orange arrows). Generalization refers to the model capability for performing well on the out-of-distribution data related to the given task, beyond the data it has seen during training (blue arrows). The sketch of the real-world strawberry in Task 1 refers to one out-of-distribution test sample, which was unseen by the model during training. Other examples for out-of-distribution data also include birds corrupted by noise or style-transferred cats. Here, we are to investigate the interplay of generalization within a given task and the forgetting about the previous tasks.

both shape and texture representation of the training images by regularizing the logits of their style transferred versions and themselves. Extensive experiments validate that our approach can be seamlessly integrated with existing continual learning methods. Its performance significantly surpasses any single continual learning baselines or their combined versions with any existing generalization methods. This highlights the effectiveness of our STCR in simultaneously improving both generalization and continual learning capabilities.

We summarize our key contributions:

- For the first time, we explored the interplay of out-of-distribution generalization of the current task and forgetting of the earlier tasks. Through a series of extensive experiments involving established generalization and continual learning baselines, our empirical evidence reveals interesting insights that generalization and continual learning capabilities are mutually beneficial.
- To enhance the generalization capabilities of existing continual learning baselines, we have developed a simple and effective shape-texture consistency regularization method (STCR). Our method distills both shape and texture representations from the training images of the current task, subsequently enhancing generalization and thereby mitigating forgetting.
- Our STCR can be seamlessly integrated with existing continual learning methods. The experimental results demonstrate significant improvements in both generalization and continual learning performances, surpassing these existing continual learning methods in isolation or when combined with established

generalization techniques.

II. RELATED WORK

A. Continual learning

Continuous learning involves acquiring knowledge in a sequential manner by training a single neural network on a series of tasks. During this process, only data from the current task is utilized for training. One grand challenge in continual learning is catastrophic forgetting [18], [19]. To tackle this challenge, the following major types of approaches have been proposed.

Regularization-based approaches [5]–[7] impose stringent constraints on model parameters. This is achieved by penalizing changes in parameters that are crucial for retaining knowledge related to older tasks. Despite demonstrating some success in alleviating forgetting, these methods fall short of delivering satisfactory performance in demanding continual learning scenarios [10], [20]. Recent approaches have incorporated knowledge distillation [21] as a regularization technique to minimize the changes to the decision boundaries of old tasks while learning new tasks. Methods based on knowledge distillation [8]–[12], typically involve maintaining a snapshot of the model trained on earlier tasks in a memory buffer. Subsequently, the knowledge encapsulated in the stored old model is distilled and transferred to the current model as part of the learning process.

Exemplar replay methods [9], [10], [13]–[16] preserve a subset of representative examples from prior tasks in a memory buffer. Many of these approaches [9], [10], [14], [15] leverage herding heuristics [22] for selecting exemplars. The stored exemplars, in conjunction with new data, are then utilized to optimize the network parameters during the learning process of a new task. While replay strategies can be notably effective, they come with certain drawbacks. The replay of a restricted set of stored examples may result in overfitting. Additionally, storing a substantial number of images for replay purposes can be memory-intensive. To address memory constraints, generative replay methods integrate data from new tasks with synthetic data generated by generative models, aiming to replicate stimuli encountered in previous instances [13], [16], [23]–[27]. Nevertheless, the generative models required for generating suitable synthetic data still tend to be sizable, memory-intensive, and challenging to train.

Dynamic architecture expansions [28]–[32] address the challenge of catastrophic forgetting by expanding the network. In this strategy, a new network is trained for each task, while the preceding networks are held constant. This ensures that the initially generated features for earlier task classes remain preserved. Despite showcasing enhanced performance compared to single-model approaches, these methods result in models that quickly escalate in size as the number of tasks increases. As a result, the scalability issue renders them impractical for many real-world applications.

Despite many of these advancements in continual learning, a predominant focus remains on testing models with in-distribution data. The generalization ability of these methods on out-of-distribution data was yet comprehensively evaluated.

In a pioneering effort, we provide empirical evidence suggesting that continual learning methods demonstrating reduced forgetting of old tasks also exhibit improved generalization for all the trained tasks.

B. Generalization

Generalization methods initially focused on increasing data diversity with augmentation techniques [2], [33]–[37]. Subsequently, researchers delved into adversarial training as a means to enhance generalization [38]–[40]. However, such adversarial training approaches often result in compromised performance within the training distribution itself [41].

An alternative avenue of research aimed at improving out-of-domain generalization involves exploring shape and texture representation learning. Geirhos et al. [36] uncovered that convolutional networks trained on natural images tend to acquire texture representations that generalize well to in-distribution data but exhibit sub-optimal performance on out-of-distribution data. In response to this, researchers have introduced methods focused on shape representation learning [36], [37], [42], often at the expense of in-distribution performance. Li et al. [1] propose shape-texture debiased training using a mixup loss to prevent bias toward either shape or texture, striking a performance balance between in-distribution and out-of-distribution data.

In contrast to existing works, our research delves into the impact of generalization methods on forgetting over a sequence of tasks within the continual learning framework. Empirical evidence from our study reveals that achieving superior generalization performance over all the trained tasks contributes to reducing forgetting for earlier tasks. In our preliminary efforts to enhance the generalization ability of continual learning methods, we introduce a straightforward yet effective shape-texture consistency regularization approach tailored for continual learning. The experimental results demonstrate that our model, serving as a plug-and-play module seamlessly integrated with any continual learning methods, outperforms various combinations of existing generalization and continual learning baselines by a substantial margin.

III. OUR PROPOSED METHOD – STCR

We present empirical evidence in **Sec. V-A** highlighting how superior generalization performance in all the tasks trained so far contributes to reduced forgetting during continual learning. To enhance the generalization capability of established continual learning methods, we introduce a straightforward and effective regularization approach, dubbed Shape-Texture Consistency Regularization (STCR). See **Fig. 2** for the method schematic. Unlike existing generalization methods, our STCR is specifically tailored for continual learning techniques. It can seamlessly integrate with any existing continual learning method. For instance, our STCR can leverage exemplars in replay-based continual learning methods to enhance generalization ability. We introduce our SGTR in this section.

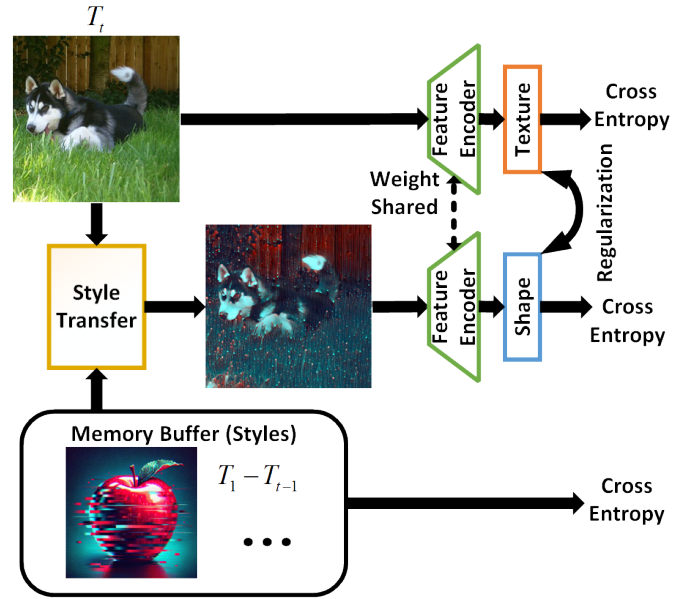


Fig. 2: Schematic of our shape-texture consistency regularization method (STCR). Given an image from the training set, we create its shape-texture conflict counterpart by performing style transfers on the training images of the current task. The style images come from the examples stored in the memory buffer. The original image and shape-texture conflict image are combined in the mini-batch for training. The feature encoder extracts both texture-biased and shape-biased representations from these mini-batches. Their output logits are then normalized for classification via cross-entropy losses. Moreover, these logits are also regularized to make consistent class distributions. During replays, the model also rehearses the old images using cross-entropy losses. By using the proposed STCR, the resulting model can effectively prevent forgetting, and meanwhile, generalize to corrupted data, and domain-shifted data during inference. See **Sec. III** for the detailed design of our STCR.

A. Problem setting

We focus on the class-incremental scenario in continual learning, where the objective is to learn a unified classifier over incrementally occurring sets of classes [14]. Formally, let $\mathcal{T} = \{\mathcal{T}_0, \dots, \mathcal{T}_T\}$ be a sequence of classification tasks, $\mathcal{D}_t = \{(x_{i,t}, y_{i,t})\}_{i=0}^{n_t}$ be the labeled training set of the task \mathcal{T}_t with n_t samples from m_t distinct classes, and $(x_{i,t}, y_{i,t})$ be the i -th (image, label) pair in the training set of the task \mathcal{T}_t . A single model Θ is trained to solve the tasks \mathcal{T} incrementally. The model Θ consists of a feature extractor and a unified classifier. For the initial task \mathcal{T}_0 , the model Θ_0 learns a standard classifier for the first m_0 classes. In the incremental step t , only the classifier is extended by adding m_t new output nodes to learn m_t new classes, leading to a new model Θ_t . During the training of Θ_t , only the training set \mathcal{D}_t for the task \mathcal{T}_t is available. In the testing phase, Θ_t is required to classify all classes seen so far, i.e., $\{m_0, \dots, m_t\}$. Unlike the existing class-incremental works, Θ_t should perform well on both the in-distribution and out-of-distribution test data. For example, if

Θ_t is trained to recognize real-world dog images, it should be capable of recognizing both real-world dog images and cartoon dog images during testing.

B. Shape-texture consistency regularization

Our STCR has to learn shape and texture representations for each classification task, enabling generalization to both in-distribution and out-of-distribution data. While standard training on natural images tends to learn texture representations for in-distribution generalization, shape representations are more robust to distribution shifts. To encourage the model to learn shape representations, we adopt the approach of Geirhos et al. [36] by using shape-texture conflict images for training. However, rather than use external artistic paintings in [36] for style transfers, we use styles from different images within the current training set \mathcal{D}_t . This is because storing paintings in memory is not feasible for memory-constrained continual learning. Specifically, during optimization at the incremental step t , we randomly sample two mini-batches of images with a size of k from the current training set \mathcal{D}_t . We use $\mathcal{X} = \{x_{1,t}, \dots, x_{k,t}\}$ as content images and $\hat{\mathcal{X}} = \{\hat{x}_{1,t}, \dots, \hat{x}_{k,t}\}$ as style images. We generate a mini-batch of shape-texture conflict images $\tilde{\mathcal{X}} = \{\tilde{x}_{1,t}, \dots, \tilde{x}_{k,t}\}$ based on \mathcal{X} and $\hat{\mathcal{X}}$, where

$$\tilde{x}_{i,t} = f(x_{i,t}, \hat{x}_{i,t}). \quad (1)$$

Here $f(\cdot)$ is the style transfer operation. Specifically, we use the real-time style transfer approach, AdaIN, which is trained using MS-COCO [43] as content images and a dataset of paintings mostly collected from WikiArt [44] as style images.

When training solely on the original natural images, the model tends to acquire texture representations. Conversely, training exclusively on shape-texture conflict images leads to the learning of shape representations. To concurrently develop both shape and texture representations, we utilize a consistency regularization approach that involves both the original natural images and the shape-texture conflict images. Specifically, let $\mathcal{X} = \{x_{1,t}, \dots, x_{k,t}\}$ be a mini-batch of k images randomly sampled from the current training set \mathcal{D}_t in the incremental step t , and $\tilde{\mathcal{X}} = \{\tilde{x}_{1,t}, \dots, \tilde{x}_{k,t}\}$ be the corresponding mini-batch of shape-texture conflict images generated following Eq. (1). Next, we obtain a new mini-batch $\{\mathcal{X}, \tilde{\mathcal{X}}\}$ by combining \mathcal{X} and $\tilde{\mathcal{X}}$ for model training. Let $\mathcal{Z} = \{z_{1,t}, \dots, z_{k,t}\}$ and $\tilde{\mathcal{Z}} = \{\tilde{z}_{1,t}, \dots, \tilde{z}_{k,t}\}$ be the corresponding logits of \mathcal{X} and $\tilde{\mathcal{X}}$, produced by the model Θ_t , respectively. \mathcal{Z} is generated using original natural images as inputs and encodes texture information. Conversely, $\tilde{\mathcal{Z}}$ is generated using shape-texture conflict images as input and encodes shape information. To ensure that the model captures both texture and shape information, we encourage \mathcal{Z} and $\tilde{\mathcal{Z}}$ to predict similar class distributions with a consistency regularization loss:

$$\mathcal{L}^{STCR} = D_{KL}(p||q) + D_{KL}(q||p), \quad (2)$$

where $p = \sigma(\mathcal{Z}/\tau)$, $q = \sigma(\tilde{\mathcal{Z}}/\tau)$, τ is a temperature hyper-parameter. We empirically set it to 2. $\sigma(\cdot)$ is softmax function. Our consistency regularization loss only requires a mini-batch of training images from the current task and it can be computed in an online manner.

C. Refinement of STCR for replay-based continual learning

Just like many existing generalization methods, \mathcal{L}^{STCR} can be integrated with any established continual learning baselines, such as EWC [5], exemplar replay [14], or knowledge distillation [8]. However, different from them, we also introduce refinements to our STCR specifically catered for replay-based continual learning methods.

In replay-based continual learning methods, exemplars stored in the replay buffer often retain additional information from earlier tasks. We capitalized on these exemplars to enhance our STCR. Specifically, instead of using styles from the current training set, we employed images from the exemplar sets as style templates to generate shape-texture conflict images. Exemplar sets encompass a broader range of classes from previous tasks, enhancing the diversity of the shape-texture conflict images. Simultaneously, these conflict images carry styles from earlier tasks, serving as a form of feature rehearsal to mitigate forgetting. In our experiments, we also observed that applying shape-texture consistency regularization during replays introduces noise from shape-texture conflict images, which can detrimentally impact replay performances (refer to Sec. V-E).

The schematic of our STCR is illustrated in Fig. 2, and its implementation is outlined in Algorithm 1. At every incremental step t , the overall loss function of STCR to train a neural network is defined as:

$$\mathcal{L}_t = \mathcal{L}_{\mathcal{D}_t, \tilde{\mathcal{D}}_t}^{CE} + \mathcal{L}_{\mathcal{P}}^{CE} + \gamma \mathcal{L}_{\mathcal{D}_t, \tilde{\mathcal{D}}_t}^{STCR}, \quad (3)$$

where cross-entropy loss $\mathcal{L}_{\mathcal{D}_t, \tilde{\mathcal{D}}_t}^{CE}$ is computed on the combination of shape-texture conflict images \mathcal{D}_t and the original natural images $\tilde{\mathcal{D}}_t$ from the current task t . For the replay-based continual learning methods, $\mathcal{L}_{\mathcal{P}}^{CE}$ is computed only on the original natural images from exemplar sets \mathcal{P} . The hyperparameter $\gamma = 0.01$ regulates the relative strength in comparison to other loss terms. We analyzed the effect of γ in Sec. V-E.

IV. EXPERIMENTAL SETUP

A. Datasets

Same as previous continual learning works [15], [16], [45], [46], we perform class-incremental experiments on three standard image datasets CIFAR-100 [47], ImageNet-100, and ImageNet-1000 [48] and follow the same training and test data splits. CIFAR-100 contains 60,000 color images with the image size of 32×32 from 100 classes, in which 50,000 images are for training and the remaining 10,000 are for testing. ImageNet-1000 contains around 1.3 million color images of size 224×224 from 1,000 classes. For each class, there are 1,300 images for training and 50 images for validation. ImageNet-100 is a subset of ImageNet-1000 with 100 classes that are randomly sampled using the NumPy seed of 1993.

Since there is a lack of out-of-distribution test sets in the existing continual learning literature, we use the datasets ImageNet-1000-C [49], CIFAR-100-C [49], and ImageNet-1000-R [50] for evaluating out-of-distribution generalization. ImageNet-1000-C and CIFAR-100-C consist of 15 diverse corruption types applied to validation

Algorithm 1: Integrate continual learning frameworks with STCR

input: \mathcal{D}_t ; /*the training set for the new task*/
require: $\mathcal{P} = \{\mathcal{P}_i\}_{i=0}^{t-1}$; /*the current exemplar sets for replay*/
require: f ; /*the style transfer model*/
output: Θ_t ; /*the new model to be learned from the new task*/

- 1 $\Theta_t \leftarrow \Theta_{t-1}$; /*add m_t new output nodes*/
- 2 construct new exemplar set \mathcal{P}_t ;
- 3 $\mathcal{P} \leftarrow \{\mathcal{P}_i\}_{i=0}^{t-1} \cup \mathcal{P}_t$; /*add \mathcal{P}_t to replay buffer*/
- 4 **for** iteration $j \leftarrow 1$ **to** l **do**
- 5 load a mini-batch $(\mathcal{X}_t, \mathcal{Y}_t)$ from \mathcal{D}_t ;
- 6 $\mathcal{X}_t \leftarrow \{(x_{i,t})\}_{i=1}^k$; $\mathcal{Y}_t \leftarrow \{(y_{i,t})\}_{i=1}^k$;
- 7 load a mini-batch $(\hat{\mathcal{X}}_t, \hat{\mathcal{Y}}_t)$ from \mathcal{P} ;
- 8 $\hat{\mathcal{X}}_t \leftarrow \{(\hat{x}_{i,t})\}_{i=1}^k$; $\hat{\mathcal{Y}}_t \leftarrow \{(\hat{y}_{i,t})\}_{i=1}^k$;
- 9 $\tilde{\mathcal{X}}_t \leftarrow \{f(x_{i,t}, \hat{x}_{i,t})\}_{i=1}^k$; /*using Eq.(1)*/
- 10 $\mathcal{Z}_t, \tilde{\mathcal{Z}}_t \leftarrow \Theta_t(\mathcal{X}_t, \tilde{\mathcal{X}}_t)$; /*forward pass for new task*/
- 11 Compute $\mathcal{L}_{\mathcal{D}_t, \tilde{\mathcal{D}}_t}^{STCR}$ with $(\mathcal{Z}_t, \tilde{\mathcal{Z}}_t)$ using Eq.(2);
- 12 Compute $\mathcal{L}_{\mathcal{D}_t, \tilde{\mathcal{D}}_t}^{CE}$ with $\{(\mathcal{Z}_t, \mathcal{Y}_t), (\tilde{\mathcal{Z}}_t, \mathcal{Y}_t)\}$;
- 13 $\hat{\mathcal{Z}}_t \leftarrow \Theta_t(\hat{\mathcal{X}}_t)$; /*forward pass for replay*/
- 14 Compute $\mathcal{L}_{\mathcal{P}}^{CE}$ with $(\hat{\mathcal{Z}}_t, \hat{\mathcal{Y}}_t)$;
- 15 $\mathcal{L}_t = \mathcal{L}_{\mathcal{D}_t, \tilde{\mathcal{D}}_t}^{CE} + \mathcal{L}_{\mathcal{P}}^{CE} + \gamma \mathcal{L}_{\mathcal{D}_t, \tilde{\mathcal{D}}_t}^{STCR}$ optimize Θ_t with loss \mathcal{L}_t ; /*backward pass*/

images of ImageNet-1000 and CIFAR-100, respectively, with five different severity levels for each corruption type. ImageNet-1000-R is a real-world distribution shift dataset that includes changes in image styles, geographic locations, etc. We curated ImageNet-100-C and ImageNet-100-R from ImageNet-1000-C and ImageNet-1000-R also by random sampling with seed 1993.

B. Protocols

We follow the standard protocols used in [11], [12], [15], [15], [16], [45], [46] for benchmarking class-incremental learning methods in continual learning. The protocol consists of an initial base task \mathcal{T}_0 followed by T incremental tasks, where T is set to 5 or 10. For all datasets, we assign half of the classes to the initial base task and distribute the remaining classes equally over the incremental steps. Additionally, we allow only 20 exemplars for each class to be stored for replay methods.

C. Metrics

For evaluation, we use the following three metrics to measure the continual learning and generalization performance:

Average incremental accuracy (Acc.) [14] is computed by averaging the accuracies of all the models $\{\Theta_0, \dots, \Theta_T\}$ obtained in all the incremental steps. Each model's accuracy is evaluated on all classes seen thus far. Acc. is a common evaluation metric in the continual learning literature, measuring the overall model performance on the in-distribution data over all the trained tasks. The higher the Acc., the better.

Forgetting (\mathcal{F}) [16] measures the performance drop of Θ_T on the initial base task \mathcal{T}_0 . It is the gap between the accuracy of Θ_0 and the accuracy of Θ_T on the same in-distribution data of

\mathcal{T}_0 . In the continual learning literature, \mathcal{F} reflects how much the model has forgotten about \mathcal{T}_0 . The smaller \mathcal{F} , the better.

Generalization (\mathcal{R} -C and \mathcal{R} -R). Here, we introduce two evaluation metrics to assess the out-of-distribution generalization capabilities of a model. This includes the robustness against data corruption and the domain shifts. Consistent with [49], we assess the robustness against data corruptions of the ultimate model Θ_T (\mathcal{R} -C) by calculating the mean corruption error across all the classes of ImageNet-100-C, ImageNet-1000-C, and CIFAR-100-C. Similarly, following the method described in [50], we evaluate the model's generalization against domain shifts (\mathcal{R} -R) with accuracy measurements on all the classes of ImageNet-100-R and ImageNet-1000-R.

D. Implementation details.

The experiments are conducted based on the publicly available official code provided by Mittal *et al.* [12]. For ImageNet-100 and ImageNet-1000, we use an 18-layer ResNet with randomly initialized weights. The network is trained for 70 epochs in the initial base task with a base learning rate of 1e-1, and is trained for 40 epochs in the incremental task with a base learning rate of 1e-2. The base learning rate is divided by 10 at epochs {30, 60} in the initial base task, and is divided by 10 at epochs {25, 35} in the incremental steps. For CIFAR-100, we use a 32-layer ResNet with randomly initialized weights. The network is trained for 120 epochs in the initial base task with a base learning rate of 1e-1, and is trained for 60 epochs in the subsequent incremental tasks with a base learning rate of 1e-2. We adopt a cosine learning rate schedule, in which the learning rate decays until 1e-4. For all networks, the last layer is cosine normalized, as suggested in [15]. All networks are optimized using the SGD optimizer with a mini-batch of 128, a momentum of 0.9, and a weight decay of 1e-4. Following [12], [15], we use an adaptive weighting function for knowledge distillation loss. At each incremental step t , $\lambda_t = \lambda_{base} (\sum_{i=0}^t m_i / m_t)^{2/3}$ where $\sum_{i=0}^t m_i$ denotes the number of all seen classes from step 0 to step t , and m_t denotes the number of classes in step t . λ_{base} is set to 20 for CIFAR-100, 100 for ImageNet-100, and 600 for ImageNet-1000, as suggested by [12]. All codes will be made publicly available upon publication.

E. Continual learning baselines

First, to demonstrate that our STCR can be integrated with any generic continual learning frameworks, we provide an overview of major frameworks used in continual learning (see **Sec.V-B**) and combine our STCR with these frameworks:

Naive trains the model on the sequence of tasks without any measures to prevent forgetting.

Weight Regularization-based (WReg). WReg-based methods are one category of continual learning methods. Elastic Weight Consolidation (EWC) [5] is one of these methods. We implement EWC, which leverages Fisher Information matrix to identify important parameters and penalizes further changes of these parameters in the later tasks.

Replay-based (Replay). Replay-based methods are the most effective group of continual learning methods. We implement

the naive replay method based on [14], which stores the images from the previous tasks in a memory buffer and replays these images together with the training images in the current task.

Knowledge distillation-based (KD). KD methods are special cases of weight-regularization methods. They turn out to be very effective, especially when they are combined with a replay-based method. We implement the knowledge distillation loss from [8], which saves a snapshot of the model in the previous tasks and distills knowledge from the old model to the new model based on the training images at the current task.

Next, to demonstrate that our STCR can further enhance the state-of-the-art (SOTA) continual learning algorithms, we integrate our STCR with three SOTA continual learning methods, each of which could incorporate a combination of multiple continual learning frameworks introduced above. We implement these approaches using their publicly available code. **CCIL** [12] employs a hybrid approach combining replay and regularization strategies.

Podnet [11] utilizes an efficient distillation loss across multiple spatial dimensions of feature maps after various pooling operations.

AFC [51] estimates the relationship between the representation changes and the resulting loss increases incurred by model updates. The greater the loss increase on the old representations, the more important the weights are to the old task. Based on the importance of the weights, the model restricts updates of important features while allowing changes in less critical features, thereby preventing forgetting.

Gdumb [52] greedily stores upcoming samples while balancing the class distribution of the memory buffer. During testing, the model is trained from scratch only using the samples in the memory buffer.

Lwf [8] is a knowledge distillation approach that regularizes the training process by aligning the predictions of the new model with those of the previous model on the new images at the current task.

iCARL [14] combines Replay and KD techniques. During training, an exemplar set of images will be dynamically selected based on feature similarity with the prototypes. Image augmentation is also applied during training and replays.

Cumulative is an upper bound. It involves training the model on all the aggregated data from $D_{t=1}$ at $T = 1$ to D_t at the current task, ensuring that the model never forgets about the old knowledge while learning the current task.

F. Generalization baselines

We compare our STCR against the following generalization approaches summarized below:

Lower bound (LB) does not use any techniques to encourage generalization.

Basic augmentation (B-Aug) follows [37] and applies simple and naturalistic augmentations, including color distortion, noise, and blur. Specifically, we employ color jitter with an 80% probability, color drop with a 20% probability, Gaussian noise (mean=0 and std=0.025) with a 50% probability, and Gaussian blur (kernel size is 10% of the image width/height) with a 50% probability.

Auto-augmentation (A-Aug) [35] represents an automated technique for identifying data augmentation strategies from the dataset, frequently resulting in improved generalization compared to basic augmentation techniques.

Style augmentation (S-Aug) [53] adopts [36] to create shape-texture conflict images using artistic painting styles and trains models on both shape-texture conflict images and original natural images. In contrast, our STCR method eliminates the need for external memory to store artistic-style images, and we introduce a regularization loss between original and shape-texture conflict images.

Mixup loss (Mixup) initially generates shape-texture conflict images by following [1] and then applies a mixup loss to these conflict images. The hyperparameter λ , determining the relative importance of shape and texture, is set to 0.8, consistent with [1].

It is important to note that our experimentation involves 4 generic continual learning frameworks, 7 continual learning baselines, and 5 generalization methods. Ideally, applying each generalization method to every continual learning baseline or framework would result in a total of $(4 + 7) \times 5 = 55$ combinations. However, due to limitations in computing resources, we pragmatically select a subset of continual learning methods and generalization methods for controlled experiments. In these experiments, we either vary the continual learning methods or vary the generalization methods, but not both simultaneously. Refer to **Sec. V** for specifications of each experiment.

V. EXPERIMENTS AND RESULTS

A. Empirical evidence on the interplay of generalization and less forgetting reveal their mutual benefits

In a pioneering effort, we investigate the interplay of generalization and less forgetting in continual learning settings on ImageNet-100 over $T = 5$. Here, we first examine how continual learning techniques, aimed at mitigating catastrophic forgetting, influence the overall generalization capabilities of models. Conversely, we delve into the impact of generalization methods on reducing forgetting across a sequence of tasks. We report both results in **Fig. 3a**.

From **Fig. 3a**, we note a strong positive linear correlation between \mathcal{F} and $R - C$ ($r = 0.93$ with a p-value of 0.01) across diverse continual learning methods. This suggests that methods exhibiting reduced forgetting also exhibit enhanced generalization capability. Essentially, a continual learning approach with diminished forgetting retains more historical knowledge, consequently augmenting the diversity of acquired features. This retained knowledge, in turn, contributes to the model's improved ability to generalize when confronted with out-of-distribution data from all previously encountered tasks.

From **Fig. 3b**, a strong positive linear correlation between $\Delta\mathcal{F}$ and $\Delta R - C$ ($r = 0.80$ with a p-value of 0.02) was observed across various continual learning methods with and without the B-Aug generalization method. This suggests that better generalization capability contributes to diminishing forgetting for earlier tasks. For instance, the Replay-based continual learning method (dark blue), incorporating the B-Aug

Method	$T=5$			$T=10$		
	$R-C \downarrow$	Acc. \uparrow	$\mathcal{F} \downarrow$	$R-C \downarrow$	Acc. \uparrow	$\mathcal{F} \downarrow$
Naive	115.88	56.45	50.04	120.71	51.16	51.07
Naive + STCR	106.68	58.64	45.44	114.54	53.94	44.16
WReg	114.94	56.70	47.72	119.05	51.68	48.88
WReg + STCR	105.47	59.47	40.32	113.42	52.78	36.64
Replay	99.69	68.29	29.56	102.62	64.69	31.68
Replay + STCR	88.79	69.51	25.84	95.88	65.89	27.92
KD	94.49	68.55	4.58	99.47	63.23	90.97
KD + STCR	82.21	70.83	3.44	90.92	64.70	3.04

TABLE I: **Generalization and continual learning performance of the generic continual learning frameworks with and without our STCR.** We reported the performance of four generic continual learning frameworks with (highlighted in gray background) and without our STCR on ImageNet-100 with $T=5$ (first column) and $T=10$ (second column) in terms of their generalization ability against data corruption ($R-C$), and continual learning ability (Acc., and \mathcal{F}). See Sec. IV-E for the introduction of these generic continual learning frameworks. See Sec. IV-C for the introduction of the evaluation metrics. The best results are in bold.

generalization method, achieves a reduction of 12.90 in \mathcal{F} and 19.46 in $R-C$ compared to its isolated counterpart. Similarly, the cumulative continual learning baseline (cyan) also experiences a substantial decrease in \mathcal{F} and $R-C$ when integrated with the B-Aug generalization method. One plausible explanation is that the generalization method empowers the model to capture more invariant and generic features in the current task, proving beneficial for both knowledge transfer to novel tasks and preserving learned knowledge from older tasks due to flatter loss minima [54].

However, we observe two exceptions in Fig. 3b. Specifically, the integration of the B-Aug generalization method has adversely affected the continual learning and generalization performances of Naive and iCaRL. Naive serves as a lower bound without any mechanisms to mitigate catastrophic forgetting. Consequently, the inclusion of the B-Aug generalization method exacerbates overfitting, resulting in a performance decline. In the case of iCaRL, where data is augmented during training and replays, the impact of the B-Aug generalization method is mitigated. In contrast to the negative effects associated with the B-Aug generalization method, our experimental results in Sec. V-D demonstrate that our STCR can even enhance the performance of the naive continual learning baseline.

B. STCL can be seamlessly integrated with any generic continual learning frameworks

Given the mutually beneficial relationship between generalization and reduced forgetting discussed in Sec. V-A, we introduced STCR as a generalization method specifically designed for continual learning (Sec. III). Here, we demonstrate that our STCR can be seamlessly integrated with any generic continual learning framework. Specifically, we selected the three most commonly used continual learning frameworks

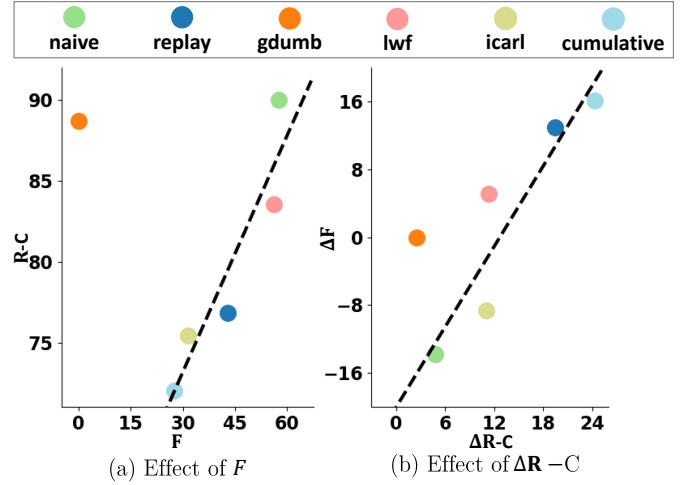


Fig. 3: **Interplay of Generalization and Forgetting in Continual Learning on ImageNet-100 when $T = 5$.** Subplot (a) illustrates the forgetting and generalization capability across a range of continual learning methods. For each continual learning algorithm, we report its $R-C$ and \mathcal{F} . We also performed a linear fitting (dashed line) between $R-C$ and \mathcal{F} based on all the sample points on the subplot using RANSACRegressor [55]. Subplot (b) presents the impact of generalization on reduced forgetting. We computed the performance difference in $R-C$ and \mathcal{F} between existing continual learning baselines with and without the B-Aug generalization baseline, and denote these differences as $\Delta \mathcal{F}$ and $\Delta R-C$. Postive $\Delta \mathcal{F}$ and $\Delta R-C$ imply that the continual learning model has improved generalization capability and reduced forgetting after integrating the B-Aug generalization algorithm, compared to its counterpart without B-Aug. The dashed line indicates the result of linear fitting between $\Delta \mathcal{F}$ and $\Delta R-C$ using RANSACRegressor [55]. See Sec. IV-E for the introduction of the continual learning baselines. See Sec. IV-F for the introduction of the generalization baselines. See Sec. IV-C for the introduction of the evaluation metrics.

as well as one naive framework (Sec. IV-E) and then applied STCR to them. These integrated frameworks are labelled as “the name of the framework + STCR”. We evaluated “framework + STCR” on ImageNet-100 with two task sequence lengths of $T = 5$ and $T = 10$ (Sec. III). For comparisons, we also evaluate these continual learning frameworks without our STCR in the same experiment settings. We report their generalization and continual learning performances in Table I.

From Table I, across both task sequence lengths $T = 5$ and $T = 10$, we observed that all the continual learning frameworks integrated with our STCR outperform their counterparts without STCR by a large margin, in terms of both generalization ($R-C$) and continual learning performances (Acc. and \mathcal{F}). For instance, when $T = 5$, WReg + STCR beats WReg alone by almost 10% in $R-C$, 3% in Acc. and 7% in \mathcal{F} . This implies that our STCR, when integrated with continual learning frameworks, is effective in enhancing generalization and reducing forgetting. Notably, STCR exhibits the capacity to reduce forgetting and enhance generalization even within

the naive continual learning framework, which lacks measures to prevent forgetting (compare Naive + STCR versus STCR).

We also found that the positive effect of STCR becomes more prominent when it is integrated with those frameworks that are better continual learners. For example, the existing works have shown that KD and Replay are the most effective strategies in reducing catastrophic forgetting, which most of the SOTA continual learning methods adopt. Indeed, compared with Naive and WReg, this is also demonstrated by higher Acc. and lower \mathcal{F} of KD and Replay as shown in **Table I**. With our STCR, the generalization performance of Replay+STCR and KD+STCR gets boosted by almost 10% and 12% compared to their counterparts respectively. This is in high contrast with a relative improvement of 7.9% and 7.8% in \mathcal{R} -C for Naive+STCR and WReg+STCR.

C. State-of-the-art continual learning methods with STCR beat their standalone configurations

In the subsection above, we demonstrated the feasibility of integrating our STCR with any generic continual learning framework. Here, we specifically assess the impact of STCR on state-of-the-art (SOTA) continual learning methods. While these SOTA methods may align with one or more of the continual learning frameworks discussed earlier, they also have distinct continual learning strategies. We highlighted these differences from the generic continual learning frameworks in **Sec. IV-E**.

In this experiment, we incorporate STCR into three SOTA continual learning methods (**Sec. IV-E**) and assess their generalization and continual learning performances across three image datasets, given two task sequence lengths of $T = 5$ and $T = 10$. The versions of the SOTA methods integrated with our STCR are labeled as “SOTA + STCR”. To facilitate comparisons, we also include the outcomes of their standalone versions without STCR. We present our results in **Table II**.

SOTA+STCR consistently outperforms SOTA themselves in terms of generalization and reduced forgetting. For instance, when STCR is applied to AFC on ImageNet-100 with $T=5$, AFC + STCR increases Acc. from 78.68 to 80.83 and decreases \mathcal{F} from 3.51 to 1.35, dramatically improving the continual learning performance. Meanwhile, AFC + STCR reduces \mathcal{R} -C by 16.7 and improves \mathcal{R} -R by 10.31, demonstrating its effectiveness in enhancing the generalization ability of these SOTA continual learning methods.

D. Continual learning methods with STCR outperform their counterparts combined with existing generalization methods

We compare our STCR and the existing generalization baselines (**Sec. IV-E**) in a continual learning setting on ImageNet-100 with $T = 5$. To isolate the effect of continual learning baselines, we use CCIL (**Sec. IV-E**) as the continual learning backbone, apply all the generalization baselines to CCIL in every task, and evaluate their performances in \mathcal{R} -C, Acc., and \mathcal{F} (**Sec. IV-C**). As controls, we also introduce the lower-bound, which is CCIL alone without any generalization methods.

We report the results in **Fig. 4**. As expected, the lower bound without any generalization methods performs the worst in terms

of all the evaluation metrics. All the generalization baselines perform slightly better than the lower bound; however, their performance is still inferior to our STCR. This implies that our STCR is more effective in boosting the generalization ability within a task, and thereby enhancing the continual learning performance with reduced forgetting.

It is also worth noting that S-Aug and Mixup share similarities with our STCR as both methods involve shape-texture conflict images. Even with the extra storage of artistic style templates, S-Aug still underperforms our STCR. This indicates that the data augmentation techniques alone are not enough. Additional regularization losses are necessary for the continual learning setting.

Moreover, in contrast to Mixup loss which balances the learnt shape and texture biases, our STCR still achieves much better performance. This suggests that our proposed consistency regularization loss is more effective than Mixup for generalization in the continual learning setting.

E. Network analysis reveals our key design decisions

To evaluate the contribution of each component in our STCR method, we repeat the experiments on ImageNet-100 using the ablated versions of our method. As control experiments, we fix the continual learning baseline CCIL ([12], **Sec. IV-E**) and use it to integrate with our ablated versions. In these experiments, the number of replay exemplars in CCIL is set to 2000. We also introduce additional application scenarios and demonstrate the benefits that our STCR can bring in these scenarios.

The effect of coefficient γ . We analyze the effect of the coefficient γ , which controls the strength of \mathcal{L}^{STCR} in **Eq. 3**, by varying its values $\gamma \in \{0, 0.001, 0.01, 0.1\}$. Note that \mathcal{L}^{STCR} is not in effect when γ is set to 0. The results, presented in Row 1-4 in **Table III**, demonstrate that incorporating STCR with small γ leads to improved performance compared to the case when $\gamma=0$, in all evaluation metrics. This suggests that the STCR is essential for enhancing the continual learning performance. We also observed that higher values of γ lead to less forgetting but may deteriorate generalization ability.

It is important to note that the impact of γ remains consistent across different learning protocols and datasets. For all protocols and datasets, we have fixed the default value of $\gamma=0.01$.

Styles from exemplar sets v.s. current training set. For replay-based continual learning methods, we emphasized the importance of using style templates from exemplar sets in the memory buffer to generate shape-texture conflict images. Here, we report the performance when the style templates come from the current training set. The results in Row 5-6 in **Table III** show that using styles from exemplar sets outperforms the one from the current training set by around 2% over the four evaluation metrics. Two possible reasons are: first, exemplar sets encompass a broader range of classes from previous tasks, enhancing the diversity of the shape-texture conflict images. Second, these conflict images carry styles from earlier tasks, serving as a form of feature rehearsal to mitigate forgetting.

STCR in replay. We investigate the impact of STCR in replays and present our findings in Row 7-8 in **Table III**. As

	ImageNet-100				ImageNet-1000				CIFAR-100		
	$R-C \downarrow$	$R-R \uparrow$	Acc. \uparrow	$\mathcal{F} \downarrow$	$R-C \downarrow$	$R-R \uparrow$	Acc. \uparrow	$\mathcal{F} \downarrow$	$R-C \downarrow$	Acc. \uparrow	$\mathcal{F} \downarrow$
CCIL [12] ($T=5$)	86.02	25.8	77.03	12.88	74.19	15.64	67.46	12.94	67.38	64.33	18.36
CCIL + STCR ($T=5$, <i>ours</i>)	69.74	40.12	79.16	7.80	69.12	19.66	67.84	10.92	62.81	65.13	13.64
Podnet [11] ($T=5$)	113.19	20.72	77.95	6.05	87.19	10.40	68.76	7.89	67.21	65.08	11.68
Podnet + STCR ($T=5$, <i>ours</i>)	100.64	27.19	78.45	4.72	81.42	13.82	69.13	7.28	66.52	65.93	9.36
AFC [51] ($T=5$)	110.53	18.44	78.68	3.51	86.74	10.37	68.75	6.85	66.83	65.80	8.17
AFC + STCR ($T=5$, <i>ours</i>)	93.83	28.75	80.83	1.35	81.24	14.72	69.48	5.70	65.66	66.07	6.55
CCIL [12] ($T=10$)	92.96	23.71	74.25	16.12	76.31	14.31	65.20	17.46	70.07	63.01	21.06
CCIL + STCR ($T=10$, <i>ours</i>)	75.45	34.58	76.72	12.60	71.92	17.84	66.47	14.31	63.83	63.69	15.94
Podnet [12] ($T=10$)	116.50	19.73	75.31	18.07	88.72	8.99	65.98	15.77	68.86	63.20	22.39
Podnet + STCR ($T=10$, <i>ours</i>)	103.00	26.72	76.11	16.41	82.41	12.85	66.32	15.50	66.99	63.69	18.13
AFC [51] ($T=10$)	112.38	19.43	76.97	13.8	89.16	7.91	67.03	13.44	68.21	64.18	16.26
AFC + STCR ($T=10$, <i>ours</i>)	95.63	25.80	79.15	12.07	82.67	12.03	68.25	12.63	67.79	64.95	12.95

TABLE II: **Generalization and continual learning performance of the state-of-the-art (SOTA) continual learning methods with and without our STCR.** We reported the performance of three SOTA continual learning methods with (highlighted in grey background) and without our STCR on two learning paradigms ($T=5$, the first six rows) and ($T=10$, the last six rows) across all three datasets (three columns) in terms of their generalization ability ($R-C$ and $R-R$) and continual learning ability (Acc., and \mathcal{F}). See Sec. IV-E for the introduction of these SOTA methods. See Sec. IV-C for the introduction of the evaluation metrics. The best results are in bold.

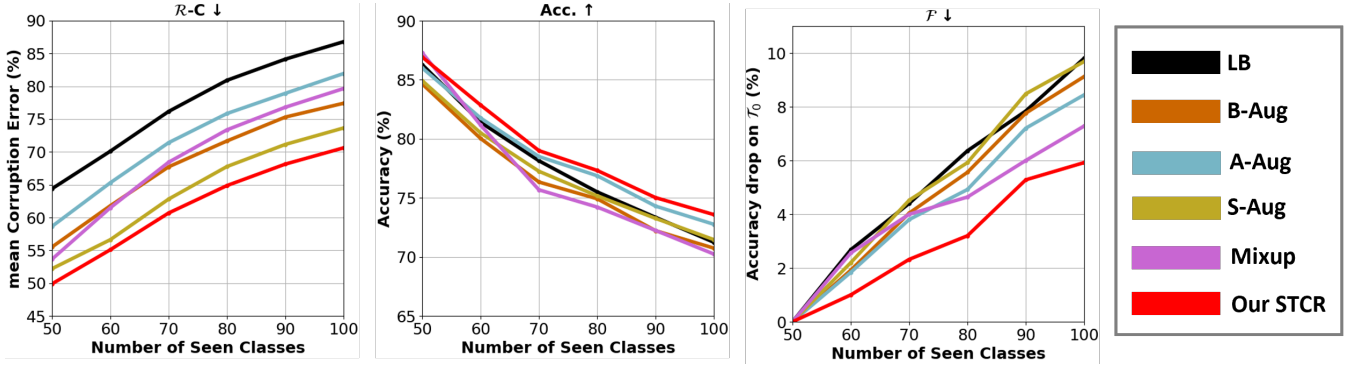


Fig. 4: **The continual learning baseline with our STCR outperforms its counterpart with existing generalization methods.** We report the generalization ($R-C$) and continual learning performances (Acc., and \mathcal{F}) of the continual learning method [12] integrated with our STCR as well as its counterpart integrated with established generalization baselines on ImageNet-100 with $T=5$. See Sec. IV-E for the introduction of each generalization baseline. See Sec. IV-C for the introduction of the evaluation metrics. The best performance is our STCR in red.

emphasized in Sec. III, performing style transfers on the replay images and training on such synthesized shape-texture conflict images during replays hinder the performance of continual learning. The synthesized images may frequently exhibit low quality, potentially due to the restricted size of exemplars in the replay buffers. Rehearsing with these images could disrupt the retention of knowledge from earlier tasks.

Longer Task Sequences. We conducted additional experiments on ImageNet-100 to evaluate the effectiveness of our STCR with longer task sequences $T=25$ and $T=50$. We evaluated CCIL ([12], Sec. IV-E) with and without our STCR in these two experiments. We presented the results in Row 9-12 of Table III. The results demonstrate that STCR can consistently improve both the generalization and continual learning performance of CCIL even over a much longer task sequence. For example, CCIL with STCR beats CCIL alone by 8% in $R-C$ and $R-R$, and 3% in Acc., and \mathcal{F} over $T=50$.

Connecting to vision transformer. We assessed the effectiveness of our STCR on continual learning methods involving vision transformer architectures [57]. Specifically, we applied our STCR on Yu *et al.* [56] (ViTIL) for training vision transformers in continual learning settings. We followed their implementation details and reported the results of their method with and without our STCR in Row 13-14 in Table III.

Consistent with the results obtained from the convolutional neural network (CNN)-based CL approaches such as CCIL [12] (see Row 15-16 in Table III), we observed improved performances of ViTIL in both generalization and continual learning evaluation metrics. Interestingly, we also noted that the performance boost in vision transformers is relatively lower than CNNs. This may be attributed to the fact that vision transformers have already learned better shape and texture representations than CNNs [58].

		$R-C \downarrow$	$R-R \uparrow$	Acc. \uparrow	$\mathcal{F} \downarrow$
COEFFICIENT	$\gamma = 0$	87.16	26.66	76.55	9.2
	$\gamma = 0.001$	68.86	38.12	77.97	8.32
	$\gamma = 0.01$ (ours)	67.59	39.53	78.76	6.92
	$\gamma = 0.1$	68.98	39.19	77.89	6.52
STYLES	current training set	70.7	38.83	77.86	8.44
	exemplar sets(ours)	67.59	39.53	78.76	6.92
REPLAY	Yes	69.68	38.45	77.58	7.95
	No(ours)	67.59	39.53	78.76	6.92
TASK LENGTH	CCIL [12] (T=25)	99.13	20.62	67.47	22.84
	w/ STCR (T=25, ours)	85.43	29.74	70.29	20.08
	CCIL [12] (T=50)	106.1	16.91	59.15	34.04
	w/ STCR (T=50, ours)	98.4	22.48	62.16	31.76
MODEL	ViTIL [56]	82.36	34.54	78.17	6.56
	w/ STCR (ours)	76.75	38.42	78.71	5.12
	CCIL [12]	87.16	26.66	76.55	9.2
	w/ STCR (ours)	67.59	39.53	78.76	6.92

TABLE III: **Generalization and continual learning performance of our STCR variations in diverse application scenarios.** We reported the generalization ability ($R - C$ and $R - R$) and continual learning ability (Acc., and \mathcal{F}) of our STCR variations in multiple scenarios on ImageNet-100. Except for the case of task lengths, we use the continual learning paradigm when $T = 5$. See Sec. IV-E for the introduction of each application scenario. See Sec. IV-C for the introduction of the evaluation metrics. The rows highlighted in gray indicate our default method design. The best results are in bold.

VI. CONCLUSION

In AI, the existing literature on generalization and continual learning has evolved independently. In our effort to bridge these fields, we presented empirical evidence showcasing their mutually beneficial relationship: effective generalization within a task facilitates quicker learning and improved performance in subsequent tasks within the continual learning framework. On the flip side, continual learning methods are designed to combat catastrophic forgetting, ensuring the preservation of knowledge from earlier tasks, and ultimately contributing to enhanced generalization for ongoing tasks. Building upon this insight, we introduced Shape-Texture Consistency Regularization (STCR), a simple yet effective regularization technique that learns both shape and texture representations for each task in continual learning. This approach integrated with any continual learning methods not only enhances generalization but also mitigates forgetting. Our extensive experiments highlight that the existing continual learning methods, seamlessly integrated with STCR, not only surpass their own performance but also outperform their counterparts integrated with any other existing generalization methods.

REFERENCES

- [1] Y. Li, Q. Yu, M. Tan, J. Mei, P. Tang, W. Shen, A. Yuille, and C. Xie, "Shape-texture debiased neural network training," in *ICLR*, 2021.
- [2] D. Hendrycks, N. Mu, E. D. Cubuk, B. Zoph, J. Gilmer, and B. Lakshminarayanan, "Augmix: A simple data processing method to improve robustness and uncertainty," *arXiv preprint arXiv:1912.02781*, 2019.
- [3] M. A. Islam, M. Kowal, P. Esser, S. Jia, B. Ommer, K. G. Derpanis, and N. Bruce, "Shape or texture: Understanding discriminative features in cnns," *arXiv preprint arXiv:2101.11604*, 2021.
- [4] A. Doerig, R. P. Sommers, K. Seeliger, B. Richards, J. Ismael, G. W. Lindsay, K. P. Kording, T. Konkle, M. A. Van Gerven, N. Kriegeskorte *et al.*, "The neuroconnectionist research programme," *Nature Reviews Neuroscience*, pp. 1–20, 2023.
- [5] J. Kirkpatrick, R. Pascanu, N. Rabinowitz, J. Veness, G. Desjardins, A. A. Rusu, K. Milan, J. Quan, T. Ramalho, A. Grabska-Barwinska *et al.*, "Overcoming catastrophic forgetting in neural networks," *Proceedings of the national academy of sciences*, vol. 114, no. 13, pp. 3521–3526, 2017.
- [6] F. Zenke, B. Poole, and S. Ganguli, "Continual learning through synaptic intelligence," in *ICML*, 2017.
- [7] R. Aljundi, F. Babiloni, M. Elhoseiny, M. Rohrbach, and T. Tuytelaars, "Memory aware synapses: Learning what (not) to forget," in *ECCV*, 2018.
- [8] Z. Li and D. Hoiem, "Learning without forgetting," *IEEE TPAMI*, vol. 40, no. 12, pp. 2935–2947, 2017.
- [9] F. M. Castro, M. J. Marín-Jiménez, N. Guil, C. Schmid, and K. Alahari, "End-to-end incremental learning," in *ECCV*, 2018.
- [10] Y. Wu, Y. Chen, L. Wang, Y. Ye, Z. Liu, Y. Guo, and Y. Fu, "Large scale incremental learning," in *CVPR*, 2019.
- [11] A. Douillard, M. Cord, C. Ollion, T. Robert, and E. Valle, "Podnet: Pooled outputs distillation for small-tasks incremental learning," in *ECCV*, 2020.
- [12] S. Mittal, S. Galesso, and T. Brox, "Essentials for class incremental learning," in *CVPR*, 2021.
- [13] A. Robins, "Catastrophic forgetting, rehearsal and pseudorehearsal," *Connection Science*, vol. 7, no. 2, pp. 123–146, 1995.
- [14] S.-A. Rebuffi, A. Kolesnikov, G. Sperl, and C. H. Lampert, "icarl: Incremental classifier and representation learning," in *CVPR*, 2017.
- [15] S. Hou, X. Pan, C. C. Loy, Z. Wang, and D. Lin, "Learning a unified classifier incrementally via rebalancing," in *CVPR*, 2019.
- [16] Y. Liu, Y. Su, A.-A. Liu, B. Schiele, and Q. Sun, "Mnemonics training: Multi-class incremental learning without forgetting," in *CVPR*, 2020.
- [17] B. Han, F. Zhao, Y. Zeng, W. Pan, and G. Shen, "Enhancing efficient continual learning with dynamic structure development of spiking neural networks," *arXiv preprint arXiv:2308.04749*, 2023.
- [18] M. McCloskey and N. J. Cohen, "Catastrophic interference in connectionist networks: The sequential learning problem," in *Psychology of learning and motivation*. Elsevier, 1989, vol. 24, pp. 109–165.
- [19] I. J. Goodfellow, M. Mirza, D. Xiao, A. Courville, and Y. Bengio, "An empirical investigation of catastrophic forgetting in gradient-based neural networks," *arXiv preprint arXiv:1312.6211*, 2013.
- [20] G. M. Van de Ven and A. S. Tolias, "Three scenarios for continual learning," *arXiv preprint arXiv:1904.07734*, 2019.
- [21] G. Hinton, O. Vinyals, J. Dean *et al.*, "Distilling the knowledge in a neural network," *arXiv preprint arXiv:1503.02531*, vol. 2, no. 7, 2015.
- [22] M. Welling, "Herding dynamical weights to learn," in *ICML*, 2009.
- [23] H. Shin, J. K. Lee, J. Kim, and J. Kim, "Continual learning with deep generative replay," *Advances in neural information processing systems*, vol. 30, 2017.
- [24] C. Atkinson, B. McCane, L. Szymanski, and A. Robins, "Pseudo-recursal: Solving the catastrophic forgetting problem in deep neural networks," *arXiv preprint arXiv:1802.03875*, 2018.
- [25] X. Liu, C. Wu, M. Menta, L. Herranz, B. Raducanu, A. D. Bagdanov, S. Jui, and J. v. de Weijer, "Generative feature replay for class-incremental learning," in *Proceedings of the IEEE/CVF Conference on Computer Vision and Pattern Recognition Workshops*, 2020, pp. 226–227.
- [26] G. Shen, S. Zhang, X. Chen, and Z.-H. Deng, "Generative feature replay with orthogonal weight modification for continual learning," in *2021 International Joint Conference on Neural Networks (IJCNN)*. IEEE, 2021, pp. 1–8.
- [27] G. M. Van De Ven, Z. Li, and A. S. Tolias, "Class-incremental learning with generative classifiers," in *Proceedings of the IEEE/CVF Conference on Computer Vision and Pattern Recognition*, 2021, pp. 3611–3620.
- [28] R. Aljundi, P. Chakravarty, and T. Tuytelaars, "Expert gate: Lifelong learning with a network of experts," in *CVPR*, 2017.
- [29] J. Rajasegaran, M. Hayat, S. H. Khan, F. S. Khan, and L. Shao, "Random path selection for continual learning," in *NeurIPS*, 2019.
- [30] C.-Y. Hung, C.-H. Tu, C.-E. Wu, C.-H. Chen, Y.-M. Chan, and C.-S. Chen, "Compacting, picking and growing for unforgetting continual learning," in *NeurIPS*, 2019.
- [31] S. Yan, J. Xie, and X. He, "Der: Dynamically expandable representation for class incremental learning," in *CVPR*, 2021.
- [32] Z. Hu, Y. Li, J. Lyu, D. Gao, and N. Vasconcelos, "Dense network expansion for class incremental learning," in *CVPR*, 2023.
- [33] H. Zhang, M. Cisse, Y. N. Dauphin, and D. Lopez-Paz, "mixup: Beyond empirical risk minimization," in *ICLR*, 2017.
- [34] T. DeVries and G. W. Taylor, "Improved regularization of convolutional neural networks with cutout," *arXiv preprint arXiv:1708.04552*, 2017.

- [35] E. D. Cubuk, B. Zoph, D. Mane, V. Vasudevan, and Q. V. Le, "Autoaugment: Learning augmentation policies from data," in *CVPR*, 2019.
- [36] R. Geirhos, P. Rubisch, C. Michaelis, M. Bethge, F. A. Wichmann, and W. Brendel, "Imagenet-trained cnns are biased towards texture; increasing shape bias improves accuracy and robustness," *arXiv preprint arXiv:1811.12231*, 2018.
- [37] K. Hermann, T. Chen, and S. Kornblith, "The origins and prevalence of texture bias in convolutional neural networks," in *NeurIPS*, 2020.
- [38] R. Volpi, H. Namkoong, O. Sener, J. C. Duchi, V. Murino, and S. Savarese, "Generalizing to unseen domains via adversarial data augmentation," in *NeurIPS*, 2018.
- [39] M. Yi, L. Hou, J. Sun, L. Shang, X. Jiang, Q. Liu, and Z. Ma, "Improved ood generalization via adversarial training and pretraining," in *ICML*, 2021.
- [40] R. G. Lopes, D. Yin, B. Poole, J. Gilmer, and E. D. Cubuk, "Improving robustness without sacrificing accuracy with patch gaussian augmentation," *arXiv preprint arXiv:1906.02611*, 2019.
- [41] D. Tsipras, S. Santurkar, L. Engstrom, A. Turner, and A. Madry, "Robustness may be at odds with accuracy," in *ICLR*, 2019.
- [42] B. Shi, D. Zhang, Q. Dai, Z. Zhu, Y. Mu, and J. Wang, "Informative dropout for robust representation learning: A shape-bias perspective," in *ICML*, 2020.
- [43] T.-Y. Lin, M. Maire, S. Belongie, J. Hays, P. Perona, D. Ramanan, P. Dollár, and C. L. Zitnick, "Microsoft coco: Common objects in context," in *ECCV*, 2014.
- [44] N. Nichol. (2016) Painter by numbers, wikiart. [Online]. Available: <https://www.kaggle.com/c/painter-by-numbers>
- [45] X. Tao, X. Chang, X. Hong, X. Wei, and Y. Gong, "Topology-preserving class-incremental learning," in *ECCV*, 2020.
- [46] A. Douillard, A. Ramé, G. Couairon, and M. Cord, "Dytox: Transformers for continual learning with dynamic token expansion," in *CVPR*, 2022.
- [47] A. Krizhevsky, G. Hinton *et al.*, "Learning multiple layers of features from tiny images," 2009.
- [48] J. Deng, W. Dong, R. Socher, L.-J. Li, K. Li, and L. Fei-Fei, "Imagenet: A large-scale hierarchical image database," in *CVPR*, 2009.
- [49] *Benchmarking neural network robustness to common corruptions and perturbations*, 2019.
- [50] D. Hendrycks, S. Basart, N. Mu, S. Kadavath, F. Wang, E. Dorundo, R. Desai, T. Zhu, S. Parajuli, M. Guo *et al.*, "The many faces of robustness: A critical analysis of out-of-distribution generalization," in *ICCV*, 2021.
- [51] M. Kang, J. Park, and B. Han, "Class-incremental learning by knowledge distillation with adaptive feature consolidation," in *CVPR*, 2022.
- [52] A. Prabhu, P. H. Torr, and P. K. Dokania, "Gdumb: A simple approach that questions our progress in continual learning," in *Computer Vision—ECCV 2020: 16th European Conference, Glasgow, UK, August 23–28, 2020, Proceedings, Part II 16*. Springer, 2020, pp. 524–540.
- [53] P. Foret, A. Kleiner, H. Mobahi, and B. Neyshabur, "Sharpness-aware minimization for efficiently improving generalization," in *ICLR*, 2021.
- [54] J. Geiping, M. Goldblum, G. Somepalli, R. Schwartz-Ziv, T. Goldstein, and A. G. Wilson, "How much data are augmentations worth? an investigation into scaling laws, invariance, and implicit regularization," in *The Eleventh International Conference on Learning Representations*, 2023. [Online]. Available: <https://openreview.net/forum?id=3aQs3MCSeXD>
- [55] S. T. Teoh, M. Kitamura, Y. Nakayama, S. Putri, Y. Mukai, and E. Fukusaki, "Random sample consensus combined with partial least squares regression," 2015.
- [56] P. Yu, Y. Chen, Y. Jin, and Z. Liu, "Improving vision transformers for incremental learning," *arXiv preprint arXiv:2112.06103*, 2021.
- [57] A. Dosovitskiy, L. Beyer, A. Kolesnikov, D. Weissenborn, X. Zhai, T. Unterthiner, M. Dehghani, M. Minderer, G. Heigold, S. Gelly *et al.*, "An image is worth 16x16 words: Transformers for image recognition at scale," in *ICLR*, 2021.
- [58] S. Tuli, I. Dasgupta, E. Grant, and T. L. Griffiths, "Are convolutional neural networks or transformers more like human vision?" *arXiv preprint arXiv:2105.07197*, 2021.